INTERNATIONAL JOURNAL FOR NUMERICAL METHODS IN FLUIDS
Int. J. Numer. Meth. Fluids 2003; **43**:577–596 (DOI: 10.1002/fld.522)

The distinctive CFD challenges of computational rheology

K. Walters[1,*,†] and M. F. Webster[2]

[1]*Department of Mathematics, University of Wales, Aberystwyth, U.K.*
[2]*Department of Computer Science, University of Wales, Swansea, U.K.*

SUMMARY

In this general lecture, we shall first outline the way computational *non*-Newtonian fluid mechanics differs from conventional computational fluid dynamics (CFD). We do this by briefly outlining the major historical developments in this relatively new field of science, which is conveniently called Computational Rheology. To illustrate essential features, we limit the discussion to the Oldroyd B, UCM and Phan-Thien/Tanner constitutive models.

In order to provide a serious challenge to existing numerical codes, we describe some recent unpublished experimental results on flow through a contraction of constant viscosity (Boger) and also shear-thinning elastic liquids. Both planar and axisymmetric contractions are of interest, and pressure drops and observed flow structures provide the relevant points of contact between experiment and numerical prediction.

Numerical codes developed at UWS involving a hybrid finite-element/finite-volume scheme for Oldroyd B and Phan-Thien/Tanner constitutive models are applied to the contraction-flow problems and an encouraging agreement is demonstrated between theory and experiment. Specifically, the dramatic experimental differences between flow in planar and axisymmetric contractions and between constant viscosity and shear-thinning polymer solutions are mirrored in the numerical predictions, at least in a qualitative sense.

Notwithstanding these encouraging developments, the review ends with a realistic assessment of the challenges still awaiting computational rheologists, with particular reference to the choice of constitutive model and the possibility of further refinements to the numerical techniques. Copyright © 2003 John Wiley & Sons, Ltd.

KEY WORDS: rheology; CFD; simulation; constitutive model; finite-element/finite-volume; viscoelastic

1. INTRODUCTION

In this presentation, our aim is to outline the distinctive computational fluid dynamics (CFD) challenges posed by Computational Rheology. Our background assumption and expectation is that the audience will have a very detailed knowledge of modern developments in CFD, but

* Correspondence to: M. Webster, Institute of Non-Newtonian Fluid Mechanics, Department of Computer Science, University of Wales Swansea, Singleton Park, Swansea SA2 8PP, U.K.
† E-mail: m.f.webster@swansea.ac.uk

Received 15 January 2003
Revised 15 January 2003

may be less aware of the novel problems which arise when the fluids are non-Newtonian and viscoelastic.

The basic challenge confronting computational rheologists is to be able to predict and simulate how *complex* non-Newtonian fluids behave when they flow in *complex* geometries. Much of the research in the field has been driven by industry, so the fluids of interest include molten plastics and polymer solutions, as well as industrial suspensions, multigrade oils, liquid detergents, printing inks and various food and confectionary products. The processes of interest include injection moulding, extrusion, coating, mixing and lubrication.

It is clear that the field is strongly motivated and is very broad in its scope. At the same time, the challenges of complex rheology turn up in most industrial processes, and we are able to be reasonably focused concerning the distinctive numerical challenges of computational rheology. Indeed, in this presentation, we purposely choose to be fairly restrictive in our choice of non-Newtonian liquids and flow geometries. We shall see that, even within this constraint, the challenges facing computational scientists are at the same time both difficult and fascinating. Certainly a simple carry-over of conventional 'Newtonian' CFD wisdom to this more general field is not possible and attempts to do so have often led to frustration and failure.

In the next section, we set the scene by describing important events in the historical development of this relatively new field, drawing heavily on a recent historical treatise by Tanner and Walters [1] (see also the popular article by Crochet and Walters [2]). We shall then outline some recent experimental data on the flow of polymer solutions through both planar and axisymmetric contractions. These surprisingly complex data provide the backdrop for our description of some recent work on CFD carried out within the University of Wales Institute of non-Newtonian Fluid Mechanics. The detailed discussion is purposely limited to those studies which directly relate to the contraction flow experiments.

The case studies chosen indicate an encouraging agreement between experiment and simulation. However, the presentation ends on a note of realism and is happy to acknowledge that many difficult challenges remain.

2. HISTORICAL DEVELOPMENTS

Before we trace in some detail the major historical developments in the field to provide a present-day backdrop, we must first highlight some popular constitutive equations for the non-Newtonian elastic liquids of interest.

In the post second-world war years, there was an initial and laudable search for constitutive equations which possessed the same level of generality as that provided by the Navier–Stokes equations for Newtonian fluids. However, it soon became evident that the equations thus derived (like those generated for the so-called 'simple fluid' of Coleman and Noll (see, for example, Reference [3]) had no hope of utility in the type of complex flow problems we have outlined. This led to some disaffected desertions, but those that remained soon realized that some compromise had to be struck between generality and tractability. So a search began for constitutive equations which were general enough to model real behaviour in simple (rheometrical) flows and yet were simple enough to allow numerical solutions to be obtained for flow in complex geometries, like those associated with contraction flows.

In the early days, the so-called upper-convected Maxwell (UCM) and Oldroyd B models became the favourites for study, partly because they were the 'bottom-line' of acceptable simplicity and also because they seemed to be able to mimic rheometrical behaviour for

a class of polymer solutions which became popular in the late 1970s and have remained so ever since. These so-called Boger fluids [4] consist of very small concentrations of high molecular weight polymers in very viscous Newtonian solvents. The attraction of these model fluids centred on the fact that they essentially possessed a constant shear viscosity η_0 in a steady simple shear flow, while at the same time being highly elastic, with a high first normal stress difference N_1 in shear flow and an extensional viscosity η_E greatly in excess of the so-called Trouton value found in Newtonian liquids (i.e. three times the shear viscosity η_0).

Interestingly, Oldroyd, who was essentially responsible for introducing both the UCM and Oldroyd B models, was Professor of Applied Mathematics at the University of Wales, Swansea, from 1953 to 1965. He had produced his classic paper [5] on constitutive modelling just before his arrival at Swansea, but he continued to produce seminal work at Swansea and a number of research students have cause to be grateful for his sympathetic and inspired supervision, including one of the present authors (KW).

In view of their historical significance and also their continued popularity in computational rheology, it is important that we introduce the Oldroyd B equation at this juncture.

Let σ_{ik} be the stress tensor, d_{ik} the rate-of-strain tensor, p an arbitrary isotropic pressure (for the *incompressible* fluids of interest here) and δ_{ik} is the Kronecker delta. The equations of state for the Oldroyd B model have the form

$$\sigma_{ik} = -p\delta_{ik} + T_{ik} \tag{1}$$

$$T_{ik} + \lambda_1 \overset{\nabla}{T}_{ik} = 2\eta_0[d_{ik} + \lambda_2 \overset{\nabla}{d}_{ik}] \tag{2}$$

where T_{ik} is known as the extra-stress tensor and the triangle signifies the non-linear upper-convected derivative introduced by Oldroyd [5] (see for example, Reference [3, Chapter 8]). The coefficients η_0, λ_1 and λ_2 are material constants. The UCM model is given by $\lambda_2 = 0$.

The equations of state for the Oldroyd B model can be written in the alternative form

$$T_{ik} = T_{ik}^{(1)} + T_{ik}^{(2)} \tag{3}$$

$$T_{ik}^{(1)} = 2\eta_0 \frac{\lambda_2}{\lambda_1} d_{ik} \tag{4}$$

$$fT_{ik}^{(2)} + \lambda_1 \overset{\nabla}{T}_{ik}^{(2)} = 2\eta_0 \frac{[\lambda_1 - \lambda_2]}{\lambda_1} d_{ik} \tag{5}$$

where f is unity for the Oldroyd B model (cf. Equation (11)). Often, the 'Newtonian' viscosity ($\mu_2 = \eta_0\lambda_2/\lambda_1$) appearing in Equation (4) is called the 'solvent' viscosity and ($\mu_1 = \eta_0(\lambda_1 - \lambda_2)/\lambda_1$) appearing in Equation (5) is accordingly called the 'polymer' viscosity.

For a steady simple shear flow with Cartesian velocity components given by

$$v_x = \dot{\gamma} y, \quad v_y = v_z = 0 \tag{6}$$

the corresponding stress distribution for the Oldroyd B model is

$$\sigma_{xy} = \dot{\gamma}\eta_0$$

$$\sigma_{xx} - \sigma_{yy} = N_1(\dot{\gamma}) = \eta_0(\lambda_1 - \lambda_2)\dot{\gamma}^2$$
$$\sigma_{yy} - \sigma_{zz} = N_2(\dot{\gamma}) = 0 \tag{7}$$

For a uniaxial extensional flow with velocity components

$$v_x = \dot{\varepsilon}x, \quad v_y = -\frac{\dot{\varepsilon}}{2}y, \quad v_z = -\frac{\dot{\varepsilon}}{2}z \tag{8}$$

the stress distribution is

$$\sigma_{xx} - \sigma_{yy} = \sigma_{xx} - \sigma_{zz} = \frac{3\eta_0[1 - \lambda_2\dot{\varepsilon} - 2\lambda_1\lambda_2\dot{\varepsilon}^2]\dot{\varepsilon}}{[1 - 2\lambda_1\dot{\varepsilon}][1 + \lambda_1\dot{\varepsilon}]} \tag{9}$$

We see from (7) and (9) that the Oldroyd B model predicts a *constant* shear viscosity η_0, a quadratic first normal stress difference N_1, a zero second normal stress difference N_2 and a potentially high extensional viscosity η_E, (indeed η_E becomes infinite at a finite value of the strain rate!). These features encouraged the use of the model in attempts to simulate the provocative experimental results on Boger fluids provided by Boger himself and others (see, for example, Reference [6]).

Integral constitutive models provide an alternative description of non-Newtonian elastico-viscous response, which is in many ways more suggestive and versatile than that provided by differential models such as (2). With this in mind, we show the equivalent integral equations for the Oldroyd B model (cf. [7]):

$$\sigma_{ik} = \frac{2\eta_0\lambda_2 d_{ik}}{\lambda_1} + \frac{2\eta_0(\lambda_1 - \lambda_2)}{\lambda_1^2}\int_{-\infty}^{t} \exp[-(t - t')/\lambda_1]\frac{\partial x_i}{\partial x_r'}\frac{\partial x_k}{\partial x_r'}\, d_{mr}(x', t')\, \mathrm{d}t' \tag{10}$$

where x_i' is the position at time t' of the fluid element that is instantaneously at the point x_i at time t.

Except for special classes of fluids such as the Boger fluids, the vast majority of non-Newtonian elastic fluids manifest a shear-thinning response in a steady simple shear flow, with the corresponding shear stress σ_{xy} being a non-linear function of shear rate $\dot{\gamma}$. The drop in viscosity with shear rate is often extravagant.

Clearly, the Oldroyd B model is incapable of simulating the behaviour of shear-thinning liquids and more complex models have to be employed. There is no shortage of contenders in this connection, but the models we shall focus upon in the present context are those associated with the names of Phan-Thien and Tanner (see, for example, Reference [8]). These so-called PTT models have constitutive equations which, *in our case*, have

$$f = \exp\left[\varepsilon\frac{\lambda_1}{\mu_1}\,\mathrm{trace}(T_{ik}^{(2)})\right] \tag{11}$$

and the same upper convected time derivative as in Equation (2).

To illustrate some of the new challenges provided by elastic liquids, we write down the governing equations for the simplest relevant constitutive model, namely the UCM model (cf. References [1] and also [9]). If u and v are the steady velocity components in the Cartesian x and y directions, we have, in the absence of body forces, the following (non-dimensional) governing equations:

$$T_{xx}\left[1 - 2We\frac{\partial u}{\partial x}\right] + We\left[u\frac{\partial T_{xx}}{\partial x} + v\frac{\partial T_{xx}}{\partial y}\right] - 2We\,T_{xy}\frac{\partial u}{\partial y} = 2\frac{\partial u}{\partial x} \tag{12}$$

$$T_{yy}\left[1-2We\,\frac{\partial v}{\partial y}\right]+We\left[u\,\frac{\partial T_{yy}}{\partial x}+v\,\frac{\partial T_{yy}}{\partial y}\right]-2We\,T_{xy}\,\frac{\partial v}{\partial x}=2\,\frac{\partial v}{\partial y} \tag{13}$$

$$-WeT_{xx}\,\frac{\partial v}{\partial x}-WeT_{yy}\,\frac{\partial u}{\partial y}+We\left[u\,\frac{\partial T_{xy}}{\partial x}+v\,\frac{\partial T_{xy}}{\partial y}\right]+T_{xy}=\frac{\partial u}{\partial y}+\frac{\partial v}{\partial x} \tag{14}$$

$$-\frac{\partial p}{\partial x}+\frac{\partial T_{xx}}{\partial x}+\frac{\partial T_{xy}}{\partial y}=Re\left[u\,\frac{\partial u}{\partial x}+v\,\frac{\partial u}{\partial y}\right] \tag{15}$$

$$-\frac{\partial p}{\partial y}+\frac{\partial T_{xy}}{\partial x}+\frac{\partial T_{yy}}{\partial y}=Re\left[u\,\frac{\partial v}{\partial x}+v\,\frac{\partial v}{\partial y}\right] \tag{16}$$

$$\frac{\partial u}{\partial x}+\frac{\partial v}{\partial y}=0 \tag{17}$$

where Re is the Reynolds number and We is the so-called Weissenberg number, given by

$$We=\lambda_1\,\frac{U}{d} \tag{18}$$

U being a characteristic velocity and d a characteristic length.

We immediately see the first major departure from the Navier–Stokes equations (which correspond to $We=0$ in (12)–(17)), namely that we are now faced with six equations in six unknowns, rather than the three in conventional CFD. In the corresponding integral formulation, there are essentially five equations in the five unknowns: u, v, p and the two displacement functions x' and y'.

One would have thought that numerical simulations for the *simplest* constitutive models would have been the most straightforward to carry out, but that has not turned out to be the case. The Oldroyd B and UCM models introduce serious numerical challenges, associated in part with their extravagant extensional viscosity behaviour and constant shear viscosity. The problems are alleviated to some extent by the use of more complicated models, such as the PTT model shown in Equation (11), which cap the extensional viscosity levels and predict shear thinning.

Interestingly, the initial enthusiasm for the use of simple Oldroyd/Maxwell models to represent the behaviour of Boger fluids has also evaporated with time (see, for example, Reference [10]), and more complicated models are now preferred for this reason also. That is not to say that simulations for simple models are out of vogue. Quite the contrary! The associated problems are still seen as significant challenges, which have to be resolved if computational rheology is to gain self-confidence and achieve scientific respectability.

Mirroring experience in many fields, initial attempts to solve rheological flow problems employed the finite-difference technique, but attention soon moved to the more versatile finite-element method, where the influence of O C Zienkiewicz was evident (as in many other related fields of course!). In recent years, spectral-element and finite-volume methods have become increasingly more popular, especially the latter. The situation that existed in the mid-1980s is captured in the text of Crochet *et al.* [9] and useful recent reviews are contained in References [11, 12].

It is undoubtedly true to say that the birth of computational rheology as we know it today can be traced to the first successful uses of *implicit* differential constitutive equations, like (2), or their integral equivalents, in the solution of non-trivial flow problems involving abrupt changes in geometry.

So far as differential models are concerned, the first successful attempts were performed for steady flows by Perera (see, for example, References [13, 14]) using finite differences and by Kawahara (see, for example, Reference [15]) who employed the finite-element technique. Solutions for integral models came later (see for example, References [7, 16, 17]).

The stage was set at this time for the dramatic surge of interest in the field which shows no sign of abating (see, for example, Reference [1, Chapter 8]). Interestingly, the first successful solutions for *time-dependent* problems were associated with University of Wales, Swansea, with the now Registrar, P Townsend, providing solutions for a problem with one space variable in 1973 and with two space variables later in 1984 [18, 19].

Looking back over the short history of computational rheology, one can pinpoint specific developments that have become major signposts. For example, the stress splitting by Perera (see, for example, References [13, 14]), for those models that do not have a readily identifiable Newtonian (solvent) contribution, was important in recovering the elliptic operator for the vorticity in the simulations. Quite simply, the extra stress tensor T_{ik} is split in the following way:

$$T_{ik} = S_{ik} + 2\eta d_{ik} \tag{19}$$

where η is a reference viscosity, and S_{ik} becomes the stress variable of relevance in the numerical codes.

In the case of abrupt changes in geometry, it was quickly realized that 'corner singularities' for elastic liquids presented significant challenges that are still not completely resolved. At the same time there have been important contributions on the subject from References [20–22]. However, we still await a convenient 'singular element' treatment that can be readily fitted into numerical codes.

A related problem is that of the thin 'stress boundary layers', which occur even in relatively smooth flow problems for highly elastic liquids (see, for example, Reference [2]).

A further complication, which is essentially suggested by experimental evidence, is that seemingly *two*-dimensional *steady* problems, like axisymmetric contraction flow, often need to be treated as *three* dimensional and *unsteady*. Of course, there are famous instances where this complication arises in Newtonian fluid mechanics; but rheology certainly adds new and provocative examples to the list.

By far the most serious obstacle to obtaining simulations for meaningful flow conditions was the so-called high Weissenberg number problem (HWNP). Referring to Equations (12)–(18) as a typical set of equations, there is a (frustratingly low) upper limit on the Weissenberg number *We* above which numerical algorithms fail. This issue bares close resemblance to the classical up-winding problem associated with the discretization of convection–diffusion equations. Here, equation-system type arises, a central theme that pervades computational rheology and separates it from classical CFD (see Section 4).

A discussion of the HWNP at an IUTAM meeting in 1978 was the basic motivation for the creation of a series of International Workshops on the Numerical Simulation of Viscoelastic Flow. These have continued at approximately 2-year intervals and still provide the focal point for discussion on challenges in computational rheology (i.e. without the need to continually

'set the scene', something which is clearly necessary in a more general conference context.) Solutions to the HWNP have gradually evolved since 1978 and the underlying causes for the breakdown are now reasonably well understood (see, for example, Reference [1]). However, that is not to say that the problem has been completely resolved! Certainly, convergence with mesh refinement is viewed as an *absolute* necessity in this connection.

3. THE CHALLENGE

To illustrate the distinctive challenges confronting computational rheologists, we shall limit ourselves to one, seemingly simple, flow regime, namely that associated with flow through contractions for highly elastic liquids. The experimental literature on the subject is vast but we would want to draw particular attention to the pioneering work of Boger, which has been well captured in a text entitled 'Rheological phenomena in focus' [6]. In the axisymmetric case, it consists of two capillaries, with an abrupt contraction between them. In the planar case, the capillaries are replaced by planar channels, which are regarded as being of infinite extent in the third dimension. The ratio between the two diameters in the axisymmetric case and the two channel widths in the planar case is called the contraction ratio, which we denote by β.

A β value of 4:1 may be regarded as having relevance in the Newtonian case, in the sense that, for ratios greater than 4:1, there are no essential changes to the flow characteristics. This is *not the* case for highly elastic liquids, and contraction ratio is found to be an important variable in the associated experiments, far in excess of 4:1.

The salient-corner vortex, which is present even in the creeping flow of Newtonian liquids, can grow in size and strength when the flow rate is increased in the case of elastic liquids, leading to the phenomenon of vortex enhancement, which can sometimes reach extravagant proportions (see, for example, Reference [6, Chapter 3]).

Often (but not always) a so-called 'lip vortex' is formed near the abrupt contraction. When this appears, it is usually a dominant influence and, on further increases in flow rate, it encapsulates the salient corner vortex, again leading to vortex enhancement.

Interestingly, for *constant-viscosity* Boger fluids, vortex enhancement is clearly evident in axisymmetric contractions, but is absent in the case of planar contractions. On the other hand, *shear-thinning* polymer solutions show vortex enhancement in both axisymmetric and planar contractions.

The whole situation is still under active experimental investigation and the challenges to computational scientists are evident. At the very least, it is incumbent on computational rheologists to be able to simulate the provocative differences between constant viscosity and shear-thinning elastic liquids and between behaviour in axisymmetric and planar contractions.

It seems that vortex enhancement is always accompanied by an extra pressure loss (over and above that expected on the basis of shear-viscosity alone). This is sometimes called the Couette correction, and it can be severe. It must be conceded that the observed large increases in Couette correction usually encountered in the case of highly elastic liquids have been reluctant to submit to numerical simulation!

It is clear that the challenges confronting CFD workers, even for relatively simple flow regimes, are non-trivial and it is true to say that progress in the area has been relatively slow.

4. SOME RECENT SIMULATIONS FOR CONTRACTION FLOWS

4.1. Background

The particular case study chosen for illustration is that of contraction flows, with a geometric contraction ratio of 4:1. Both sharp and rounded corners are considered under planar and axisymmetric configurations.

Reviewing the expansive literature on contraction flows, we consciously restrict attention principally to the creeping flow of Oldroyd-B fluids through planar abrupt 4:1 contractions (with sharp re-entrant corners). We begin by first citing two valuable contributions from Marchal and Crochet [23, 24], with a coupled finite-element scheme, a steady formulation, and a Newton–Raphson iteration. Hermitian elements were introduced in the 1986 paper and found to enhance the limit of convergence in De (to 7.39) over a more conventional Lagrangian element choice (which gave a limit of Deborah number $De=2.1$).[‡] The Hermitian approach includes continuous representation for velocity gradients. A lip-vortex was detected with the Hermitian scheme at $De=3.2$, that increased by a factor of 5 in intensity at the higher value of $De=6.04$. An increasing trend was also observed for the salient corner vortex over the same range of De. In the subsequent 1987 article, with inconsistent streamline upwinding (SU) and 4×4 linear stress sub-elements, steady solutions were achieved up to a De of 20 without loss of convergence. The SU method provided only the onset of a weak lip vortex at $De=7.6$. This was considered a numerical artefact by the authors, as the feature disappeared with increase of De to 14 and above. The size and intensity of the salient corner vortex remained weak and insensitive to increasing elasticity.

Luo and Tanner [25] compared Galerkin, SUPG and SU methods for this problem using a decoupled finite-element approach, concentrating on accuracy and convergence behaviour of the different solutions. A full viscous splitting was also adopted in the momentum equation. The SU method (with 4×4 stress sub elements) was again observed to reach the largest De values, yielding smoothed solutions with enhanced stability, though inconsistency effectively altered the constitutive model (and hence the problem). Their observations on a single mesh were that, with increasing De, there was no evidence of a lip vortex, and that the salient corner vortex remained weak in size and intensity.

Lip vortices were also observed with a finite-volume scheme implemented by Yoo and Na [26]. This involved a version of the SIMPLER algorithm based on a staggered grid system. With increase in De, the lip vortex increased in size and intensity. The salient corner vortex was hardly influenced by increasing De, though its centre of rotation was shifted towards the slit entrance. This technique realised a critical De of 3.1. The effect of adding inertia was also noted, whereupon the vortices decrease in size and strength, though lip vortices still persist. Salient corner vortices were compressed further into the corner recess with increase in flow rate. At low elasticity, the lip vortex was segregated from the salient corner vortex, whilst, at higher elasticity, lip and salient vortices co-exist within a single recirculation cell.

Transient schemes for this benchmark problem have been investigated by Sato and Richardson [27], Basombrio *et al.* [28], Baaijens [29] and Olsson [30]. The work of Sato and Richardson is based on a hybrid finite-element/volume method with a pressure–correction

[‡]In the present context, the Deborah number can be seen as an alternative to the Weissenberg number We with the same essential definition, noting the scale conversion $De=6\,We$ for planar flows.

scheme and a time-stepping procedure. They observed a lip vortex as a pseudo-transient phenomenon that appeared at $Re=0.01$, being induced by an instantaneous increase in De from 6 to 12. The lip vortex then disappeared through the time-stepping process as a steady state was approached at the limiting value of $De=12$. Olsson [30] also observed a similar trend in a transient (iterative) appearance and disappearance of a lip vortex for a Giesekus fluid with a rounded corner, using a method-of-lines time-integration technique and a finite-difference discretization. Sato and Richardson conducted additional tests at $Re=1$ and 0.1, and provided a graph of comparative performance of corner cell vortex size from the relevant literature. Sato and Richardson comment, that at $Re=1$, the onset of a steady lip vortex was sensitive to the mesh size in the re-entrant corner neighbourhood, only being detected on their finest mesh at $De=12$. Data for $Re=0.01$ tend to align closely with the creeping flow results, whilst the $Re=1$ results were found to reduce the detachment length. At fixed Re, there is a general trend of marginal decrease in detachment length with increasing De. This is demonstrated more clearly in the accurate results reported in References [31, 32].

Basombrio *et al.* [28, 33] have also studied the creeping-flow problem using a transient decoupled method based on a Lagrange–Galerkin technique for velocities and a Lesaint–Raviart discontinuous method for stresses using linear shape functions. This is a modified version of the Fortin and Fortin [34] approach that employed quadratic shape functions. The work of Fortin and Pierre [35] has shown that for the viscoelastic Stokes problem there is, in addition to the standard Babuska–Brezzi condition, a further compatibility relationship that should hold between the trial spaces in a velocity–pressure–stress formulation. This requires that the gradient of the velocity space should lie within that of the stress space. Recovery satisfies this requirement at the continuous level. A discontinuous stress approximation (such as DG), also satisfies this compatibility condition. Basombrio *et al.* [28, 33] investigated the incorporation of SU smoothing for stress, noting that its inclusion significantly influences the size and intensity of the salient corner vortex at a value of $De=18$. Longer geometry lengths were thought necessary to proceed further in convergence to larger values of De. The SU version yields a large vortex, which is at variance to the above-cited results. Also this linear interpolation method was compared against a characteristic-based algorithm of Basombrio [28, 33] using quadratic interpolation. The quadratic form hinted at a minuscule lip vortex at $De=6$, but subsequently failed to converge for a De of 6.07, whilst the linear alternative was able to reach the elevated value of $De=18$, but without generating lip vortices. Baaijens [29] employed a space–time/Galerkin least squares technique with discontinuous stress. Here, a limiting De number of 10 was observed. A stress variable transformation similar to that employed in the EVSS formulation was used, though no mention was made of vortex behaviour.

Keiller [36] selected a related problem to study—that of sink flow into a channel with a rounded corner. This analysis is useful as it pinpoints vortex activity near the corner, in isolation from salient-corner vortex activity, and removes the uncertainty associated with solution singularly at the re-entrant corner. Both planar and axisymmetric flows were considered using a fourth-order differential stream function formulation, a finite-difference discretization, and a decoupled method of solution. Results were presented for Oldroyd-B and FENE models, and a full viscous stress splitting was employed in the momentum equation. A time-stepping technique was used as an iterator for the constitutive equation. No vortices were observed in Oldroyd-B solutions up to the limiting value of $De=24$, though they did appear in the corner neighbourhood with the FENE model at around $De=36$. In contrast, for axi-symmetric

flows, a vortex was first detected at $De=16$ for the Oldroyd-B model. We note in passing that nonlinear models that display some constraint on extensional behaviour, such as the Phan-Thien/Tanner and FENE models, have been shown to overcome moderate limiting De convergence constraints for such complex flows.

Purnode and Crochet [37] have produced some recent simulations with FENE models that compare well with experiments for planar contraction flows. Good correlation was achieved in their shear-thinning results for sharp and rounded corners.

Mitsoulis, in a series of articles (see for example, References [38, 39]), has employed integral K-BKZ (multi-mode) models, mainly for axisymmetric flows, for different contraction ratios and representing different fluid rheology. For the 4:1 axisymmetric contraction, monotonic increase of vortex size with flow rate (De) was observed and the rounded corner reduced the size of the vortex substantially. Overall, it was claimed that the integral K-BKZ model captured experimental flow behaviour fairly well.

In the recent work of Matallah *et al.* [40], with Oldroyd-B models, the numerical algorithm featured an SUPG finite-element method with velocity gradient recovery for the constitutive equation. Both sharp and rounded-corner problems were addressed. For the sharp-corner case, a lip vortex appeared at $We=1$, and grew in intensity with increase in elasticity. Nevertheless, mesh refinement minimised such lip vortices, practically removing them up to $We=2$. Baloch *et al.* [41] and Matallah *et al.* [40] showed that inertia, at a level of $Re=1$, tends to suppress the salient corner vortex both in size and strength, and likewise any appearance of a lip vortex. In contrast, for the rounded-corner problem, no lip vortex was observed and the salient-corner vortex was suppressed.

Carew *et al.* [42] selected both Oldroyd-B and linear PTT models to solve the 4:1 sharp-corner problem, with the inclusion of inertia ($Re=1$). For $\varepsilon=0.02$ in the PTT model, a lip vortex appears at $We=5$, engulfing the salient corner vortex at $We=10$, to eventually present a single vortex at $We=15$. In contrast, without inertia, no lip vortex was apparent at $We=5$. Also, for $\varepsilon=0.25$ and $We=10$, no evidence of a lip vortex was reported.

Recent work in finite-volume discretization reflects these finite-element findings. Phillips and Williams [43] reported lip-vortex activity for the flow of an Oldroyd-B fluid through a 4:1 abrupt planar contraction, for $We>2$. Alves *et al.* [44] reached identical conclusions for UCM fluid in the same geometry, as did Aboubacar and Webster [31] and Xue *et al.* [45] for an Oldroyd-B model ($We>1$). Mesh refinement has been a highly prominent feature in these studies, yielding an accurate and reliable representation of vortex structure.

4.2. Application to the local scheme

Galerkin methods are optimal for self-adjoint problems and are ideal for the discretization of elliptic operators. In contrast, finite volume methodology has advanced considerably over the last decade, supplanting finite differences in their treatment of conservation laws. This includes pure advection equations, and hence, have application to hyperbolic equations of first order in space and time. In this area, we may cite the seminal studies on cell-vertex fv schemes by Morton and co-workers see (for example, References [46–49]). These authors have championed such formulations for advection, Euler and compressible Navier–Stokes equations. In contrast to their cell-centred counterparts (cf. Reference [50]), cell-vertex schemes have been shown to be less susceptible to spurious modes, and importantly, maintain their accuracy for structured and unstructured meshes. The study of viscoelastic flow with differential

constitutive models introduces mixed-type coupled differential systems with non-trivial (solution-dependent) stress source terms. The approximation of such source terms presents some provocative new challenges to fv methodology. They may dominate in some sections of the flow. This stands in stark contrast to the context of pure advection, for which classical fv theory has been derived. These source terms, themselves depend upon velocity gradients, making their accurate resolution crucial to the process as a whole.

Bearing these issues in mind, the underlying theme of the current preferred approach is to apply finite element (fe) methodology to the self-adjoint sections of the system, and finite volume (fv) schemes to the hyperbolic parts: a hybrid formulation. As such, the numerical simulations in this review are performed through a novel finite volume/element scheme (fe/fv) first proposed in Reference [51] and further refined in Reference [52]. New aspects of this approach for viscoelastic flows include: the hybrid formulation itself; cell-vertex positioning of variables, fv approximation on triangles and sub-cells; inclusion of solution-dependent source terms; and consistent treatment for stress terms (flux, source and time terms, as with fe Petrov–Galerkin variational weighting).

A drawback to earlier fv-schemes for viscoelastic flows has been their low order of approximation; their advantage lying in efficiency. The favoured hybrid fe/fv spatial discretization has been established as a second-order scheme, with some improved properties over a pure fe counterpart. This scheme combines a cell-vertex finite-volume scheme for the differential constitutive laws with a finite-element discretization (semi-implicit Taylor–Galerkin/Pressure–Correction) for the mass and momentum balance sub-system. The combination forms a time-stepping process, with a fractional-staged formulation based upon each time step, invoking two-step Lax–Wendroff and Crank–Nicolson procedures. Four linear finite-volume triangular cells are formed as embedded sub-cells of each parent quadratic finite-element triangular cell, connecting the mid-side nodes of the parent cell. Here, we note the association with super-convergence points (cf. Reference [40]). A similar sub-cell reference was implemented by Marchal and Crochet [24] in the fe-context. Stress variables are located at the vertices of the finite-volume cells and may be used directly, without interpolation, as fe nodal values. Fluctuation distribution for cell-vertex fv schemes refers to the upwinding technique that distributes control volume contributions for each equation to provide nodal solution updates. For the stress nodal update, we consider a fluctuation distribution contribution over the fv-triangle, and a uniform distribution over the median dual cell. The latter is a unique non-overlapping region associated with each finite-volume node, a new concept arising with cell-vertex schemes.

This cell-vertex finite-volume sub-element approach has proved itself to be an effective strategy through the judicious discrete treatment of flux, source and time terms of the constitutive equation. Consistency was observed to be a key aspect. This work was novel in the cell-vertex context, as initial developments for flux distribution were solely for pure advection problems, considered here under extension with source terms. Second-order accuracy was also achieved by appealing to the parent finite-element solution representation in evaluation of the sub-cell finite-volume integrals. Wapperom and Webster [51] recognized the importance of linearity preservation to achieve high-order accuracy and Chandio and Webster [53] the role of positivity in transient stability. Our prior studies have established accuracy properties against analytical solutions for smooth model problems, and addressed stability issues for complex smooth and non-smooth flows [51, 52].

Cross-reference is made to the hybrid fe/fv study of Sato and Richardson [27] for its similarity in philosophy, the articles by Tanner and co-workers (see, for example References

[54, 55]), with artificial stress diffusion, and the discontinuous Galerkin and Galerkin least square approach of Baaijens [11]. Under such discontinuous stress representation (with correspondence to fv weighting), we also note the work of Fortin and Fortin [34] with discontinuous quadratic interpolation and Basombrio *et al.* [28, 33] with discontinuous linear interpolation. The studies of Baaijens are useful for two reasons: they point to various alternative additional stabilisation possibilities from a Galerkin least-square approach, that may be incrementally incorporated consistently into the formulation; also there is the strain-rate smoothing for momentum.

The literature on fv implementations for viscoelastic flow splits into treatments of the full system through fv and hybrid versions. We refer to Reference [51] for a review and highlight the related hybrid scheme of Sato and Richardson [27] which employed a time-explicit fe method for momentum and time-implicit fv for pressure and stress of cell-centred type. Higher-order upwinding was achieved through application of a TVD flux-corrected (inconsistent) transport scheme to the advection terms of the stress equation, addressing the complication of flux–source interaction in the presence of highly elastic convection. Most fv implementations consider established standard low-order discretization, with cell-centred or staggered grid systems, and SIMPLER-type algorithms for steady-state solutions on structured rectangular grids. (See the work of Tanner, Phan-Thien and co-workers who incorporated a stabilizing artificial stress diffusion, reminiscent of the SU method of Marchal and Crochet.) Such discretization essentially implies piecewise constant interpolation.

Phillips and Williams [43] and Alves *et al.* [44] are two recent papers that adopt the SIMPLER-type full system fv approach for the abrupt 4:1 planar contraction flow using staggered grid systems. For an Oldroyd-B fluid Phillips and Williams used a first-order implementation that applies a semi-Lagrangian treatment for convection terms. This avoids the calculation of normal stresses at the re-entrant corner. For corner shear stress, an averaging procedure was applied. With mesh refinement, it was shown that the size of the salient corner vortex remained fairly constant, in agreement with Matallah *et al.* [40] and Sato and Richardson [27], both for creeping flow and with inertia ($Re=1$). On coarse meshes, Phillips and Williams noted an absence of lip-vortex activity. In contrast, on their finest mesh, a lip vortex appeared around $We=2$ and grew as the level of fluid elasticity increased up to a maximum value of $We=2.5$.

For the same flow and a UCM fluid, Alves *et al.* compared first-order and second-order schemes. The Alves *et al.* discretization avoids placing any stress variable at the re-entrance corner. Their first-order implementation was able to converge up to $We = 8$ on a refined mesh, but proved inaccurate, reflecting a large spurious vortex structure. An alternative second-order scheme failed to converge at Weissenberg numbers above unity on the same refined mesh. This premature breakdown in numerical convergence (inhibiting advance in We) was noted by Alves *et al.* to correspond to oscillations in the stress field. These oscillations are associated with the use of high-order upwinding in regions of high stress gradients, and are overcome by applying a limiting (min-mod) procedure to the stress convection (see also, Reference [27]). In this manner, Alves *et al.* were able to reach a Weissenberg number of 3 on their finest mesh.

Most recently, the UWS work has led to an optimal implementation of this fe/fv scheme. This involves, amongst other things, a linear representation of the stress, based on the fv sub-cell with a non-recovered (multi-valued) stress gradient, constant per sub-cell. Velocity gradients are chosen of quadratic form over the parent finite-element (akin with velocity fields).

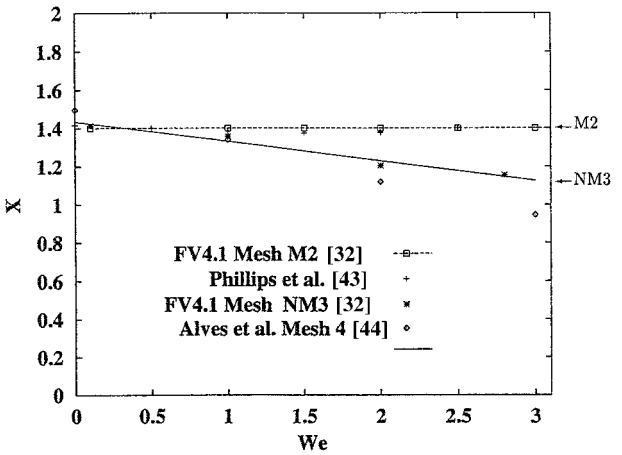

Figure 1. Numerical results for the size of the salient-corner vortex for the Oldroyd B model in a sharp corner 4:1 contraction.

A principal issue has been the recognition of the powerful influence that non-conservative area integral representation has on R_T. This stands in striking contrast to conventional fv-methodology, where conservative line integrals are preferred (such as in cell-centred approaches). In this respect, it is effective to invoke multi-valued stress gradients. Lastly, in the vicinity of sharp gradients, one can appeal to a local treatment to allow for some degree of discontinuity, that is, say, through reduced corner integration (RCI) sampling. The combination of these specific options generates the recommended fv-schemes, covered in some detail elsewhere [31].

4.3. Some numerical simulation results for contraction problems

Using the hybrid UWS fe/fv scheme, we provide a sample of results for the benchmark problem of contraction flow. We restrict ourselves here to a 4:1 contraction ratio, but take this under sharp and rounded-corner instances, for both planar and axisymmetric configurations. We present the corresponding solutions through streamline patterns to focus attention on the all important issue of vortex behaviour with parameter variation. Results are presented through increasing Weissenberg number for creeping-flow conditions. This may be interpreted as increasing the flow rate (shear-rate) for a fixed fluid, or increasing the fluid elasticity at a fixed flow rate. To compare with experimental findings the former view is appropriate. Rheological aspects involve predictions for viscoelastic models of the Oldroyd-B type, with constant shear viscosity (used to represent Boger fluids), and for shear-thinning Phan-Thien/Tanner models.

The important interrogation of solution quality with respect to mesh refinement (accuracy) has been dealt with elsewhere in precursor articles, on the sharp-corner planar contraction flow for Oldroyd models and with respect to the rounded-corner alternative for Oldroyd-B and Phan-Thien/Tanner models. In planar sharp-corner studies for Oldroyd models, a four-tuple set of meshes reveals that consistency and accuracy is vital to the correct detection of such solution features as lip-vortex onset and salient-corner vortex cell-size (X). So, for example, spurious lip vortices (numerical artefacts) were observed for $We = 1$. These diminish and

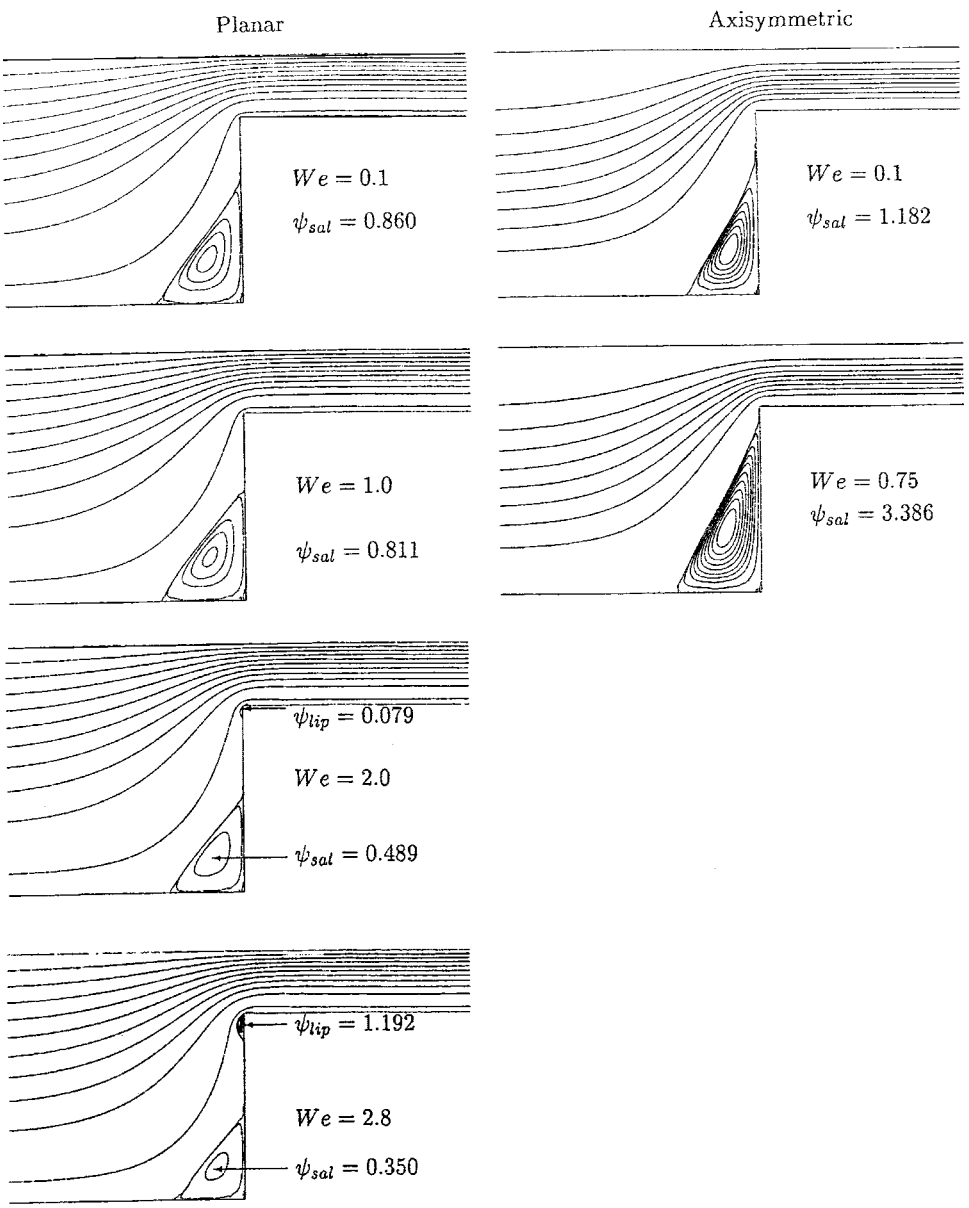

Figure 2. Streamlines in planar and axisymmetric 4:1 contractions for an Oldroyd B model on the finest mesh.

practically vanish at $We = 2$ with mesh refinement, but lip-vortex presence is in evidence beyond $We = 2$ on the finest meshes (mesh NM3). Clearly, great care is demanded here to make definitive statements, particularly in the light of the re-entrant corner solution singularity and the presence of sharp stress downstream boundary layers. This issue has arisen many times in

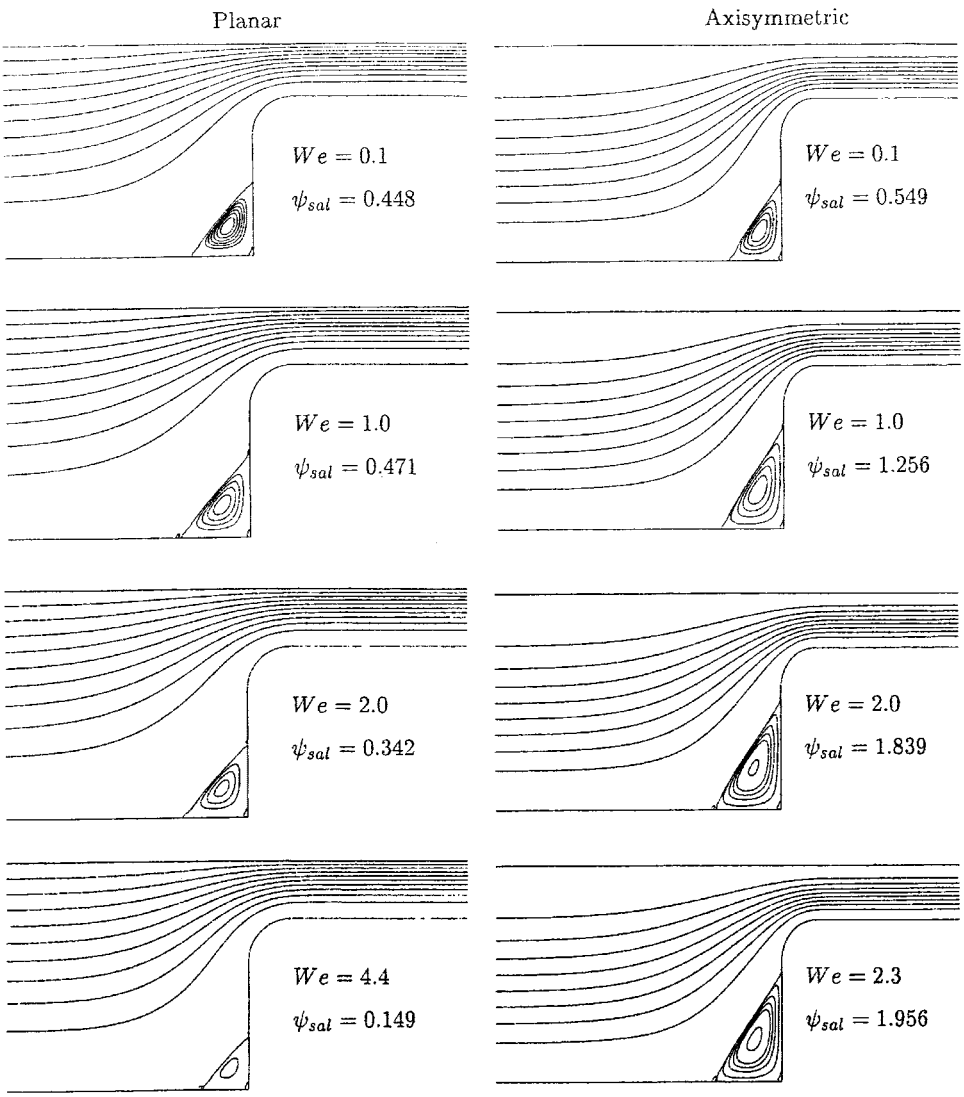

Figure 3. Streamlines in planar and axisymmetric smooth corner 4:1 contractions for an Oldroyd B model on the finest mesh.

the literature, as cited above. The precise recording of vortex trends, enhancement or inhibition, is made through measures such as the salient corner vortex cell size, the non dimensional length between the salient corner and the vortex separation line intersection with the upstream wall. For this problem on coarser meshes, X has widely been reported as remaining constant around 1.4 with increasing elasticity. On finer meshing, however, vortex reduction is observed, of order of 20% as We approaches 3. The relevant numerical simulations are given in Figure 1.

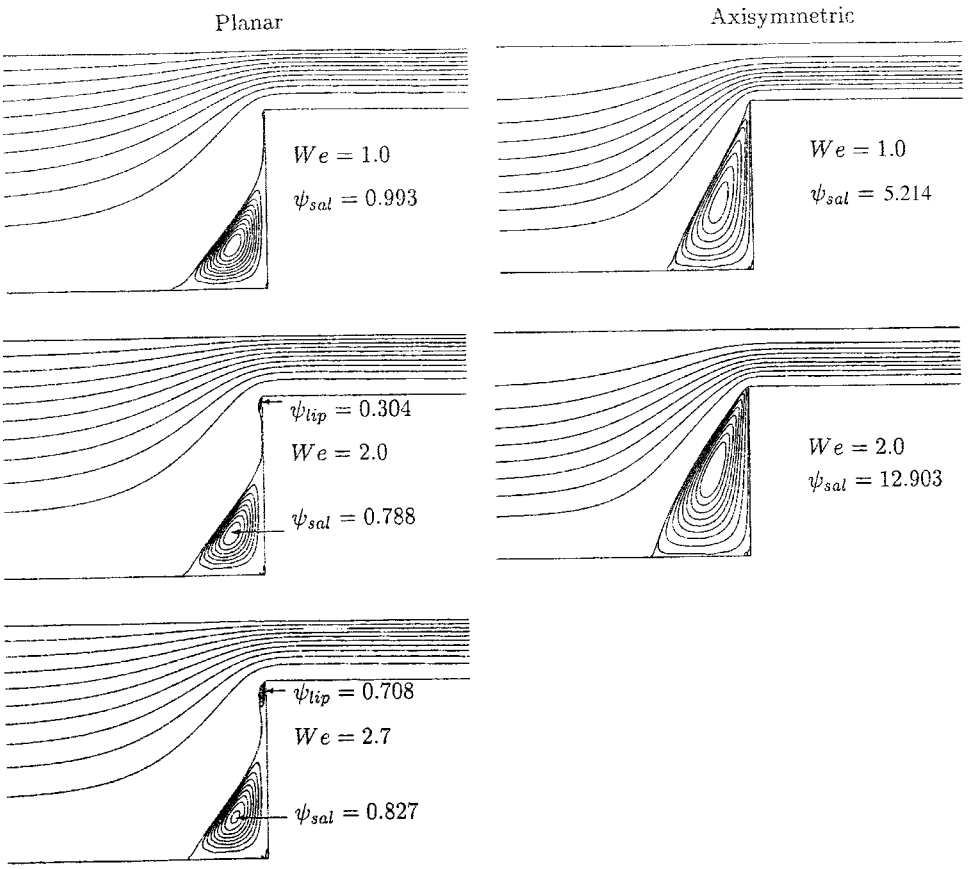

Figure 4. Streamlines in planar and axisymmetric sharp-corner 4:1 contractions for a PTT model with $\varepsilon = 0.02$.

Next, we present in Figure 2 samples of streamline patterns for the Oldroyd-B model and the sharp-corner geometry, with rising levels of *We*. All results correspond to the choice of the finest meshes employed.

The order of presentation permits unambiguous comparison between planar and axisymmetric flows at equivalent parameter settings. We observe that salient-corner vortex inhibition is apparent for planar flows, as is particularly prominent beyond a *We* of unity to the limiting We_{crit} level of 2.8. The converse is true for axisymmetric flows, in which vortex *enhancement* is noted, signalled through size and strength. This occurs somewhat earlier in the *We* range compared to planar flows. Here, salient-corner vortex intensity is some 3 times larger than that for the planar flow. This finding follows the experiments for Boger fluids, reported in Section 3. There is clear evidence of the corner lip vortex in the planar flow, beyond a *We* of 2. This is absent from the axisymmetric flow, though the level of We_{crit} is more restrictive than in planar.

Switching to the rounded-corner geometry in Figure 3 the above comments on salient-corner vortex behaviour are re-echoed. In the absence of a corner solution singularity, levels of

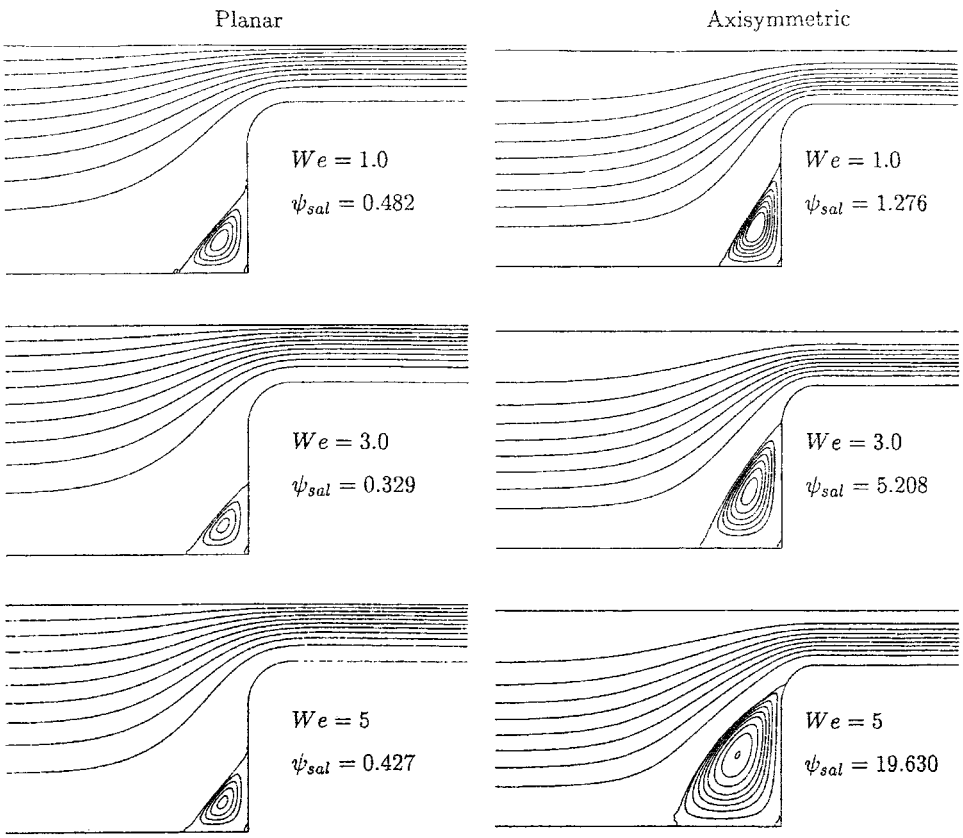

Figure 5. Streamlines in planar and axisymmetric rounded-corner 4:1 contractions for a PTT model with $\varepsilon = 0.02$.

We_{crit} are raised so that wider ranges of We values are accessable. Planar flow reflects vortex inhibition beyond a We of unity; axisymmetric flow again manifests vortex enhancement with a We_{crit} of 2.3. For rounded-corner flows and Oldroyd models, no lip-vortex activity is detected. Also, since the limiting levels of We are relatively low for the Oldroyd model, vortex intensities are not so excessive and curvature of the separation streamline is barely evident, irrespective of planar or axisymmetric considerations, or corner shape.

For the PTT model considered in Figures 4 and 5, shear thinning is introduced. In addition, for the conditions we have taken, the uniaxial extensional viscosity adopts a complicated form, reflecting strain hardening at low extension rates (0(1)) but shifting to a strain-softening form for deformation rates beyond this level. The strain-hardening response is similar to that of the Oldroyd model at finite strain-rate levels. This is often held responsible for the premature termination of numerical convergence and the manifestation of the subsequent problems that arise due to instability.

For the sharp-corner flow shown in Figure 4, vortex inhibition is again initially in evidence for the planar version. This is only slight and occurs whilst We rises to 2. Beyond this stage, vortex strength slightly increases up to a We_{crit} of 2.7. A lip-vortex is again in evidence at

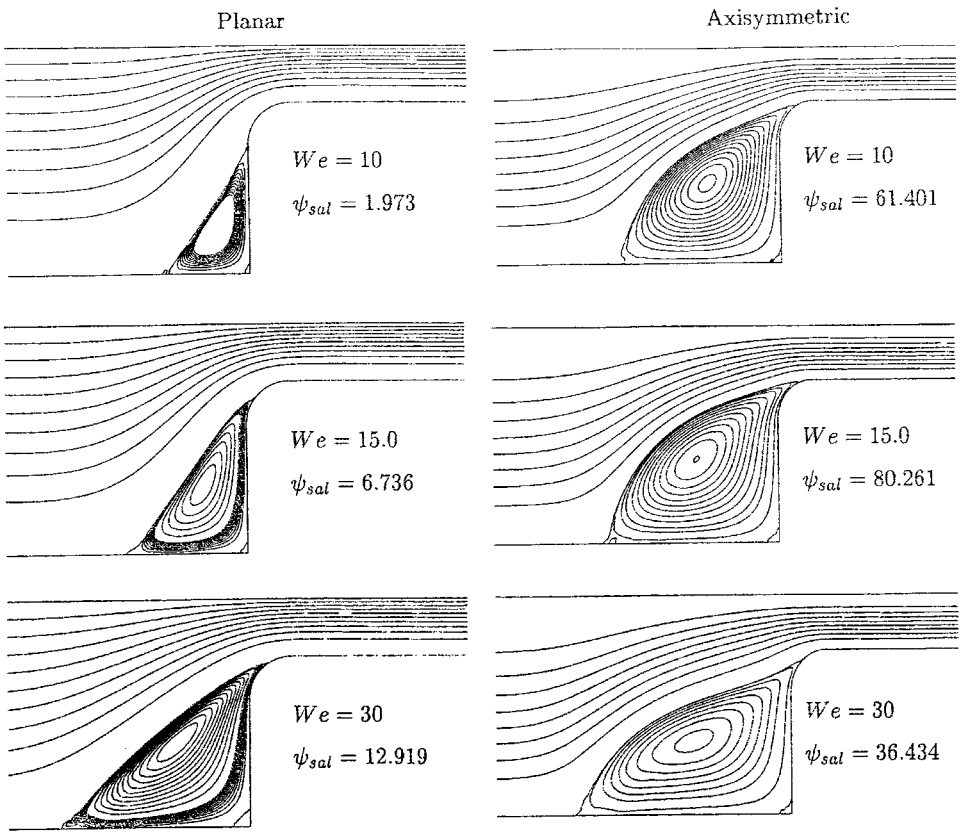

Figure 6. Streamlines for high *We* in planar and axisymmetric rounded-corner 4:1 contractions for a PTT model with $\varepsilon = 0.02$.

and beyond a *We* of two. There is some indication of concave separation line curvature within these patterns. The axisymmetric counterpart problem is distinctly different in flow structure. A large recirculation region is present at a *We* of unity, occupying the whole region from salient to re-entrant corner. With a rise of *We* to 2, a critical level, massive vortex intensity ensues (13 times greater than that at $We = 1$) and the separation streamline displays convex shape.

The rounded-corner flow considerably expands the *We* range, by at least an order of magnitude, to a We_{crit} of 30 (see Figures 5 and 6). This permits a much richer scenario to emerge. Generally, one observes significantly larger vortices in the axisymmetric over the planar flows and no lip-vortex activity is apparent in either. For the planar case, vortex reduction occurs for a *We* up to around 3, but by a *We* of 10, vortex enhancement is already quite striking. This trend continues, rising sharply at a *We* of 15–30. The concave shape of the separation streamline is lost around a *We* of 15, turning to convex by the level of 30, with a distinct fingering trend around the rounded-corner. The axisymmetric flow reflects major vortex enhancement with *We* increase, even for *We* levels lower than 3. Major increments are observed in vortex strength between 3, 5, 10 and 15, with convex separation line curvature appearing

at a *We* of 5. Fingering to and around the corner has occurred by a *We* of 10. Beyond a *We* of 15–30, vortex intensity halves, though cell-size itself increases.

The important new information that the PTT model results provides, above those for the Oldroyd B model, lies in the significant vortex enhancement attainable in both axisymmetric *and* planar contractions. This is most apparent in the rounded-corner flows that yield significantly wider *We* ranges.

We see that the trends in the numerical simulations are in encouraging agreement with the experimental data discussed in Section 3.

5. CONCLUSION

Much progress has been made in recent years in the numerical simulation of non-Newtonian flow. We have illustrated some of these encouraging developments by considering flow in planar and axisymmetric contractions for both constant viscosity and shear-thinning elastic liquids. Numerical simulation has been able to mirror and capture the quite dramatic features found in the experiments.

Of course, the constitutive models we have employed are known to be too simple to represent the behaviour of the real liquids quantitatively. Also, we have not studied the provocative effects that are known to occur when the contraction ratio is changed in the experiments. Finally, there remains the frustrating limitations on the Weissenberg number in the simulations.

There is clearly much work still to be done, but recent progress has been encouraging.

REFERENCES

1. Tanner RI, Walters K. *Rheology*: *An Historical Perspective*. Elsevier: Amsterdam, 1998.
2. Crochet MJ, Walters K. *Endeavour* 1993; **17**:64.
3. Barnes HA, Hutton JF, Walters K. *An Introduction to Rheology*. Elsevier: Amsterdam, 1989.
4. Boger DV. *Journal of non-Newtonian Fluid Mechanics* 1977/78; **3**:87.
5. Oldroyd JG. *Proceedings of the Royal Society A* 1950; **200**:523.
6. Boger DV, Walters K. *Rheological Phenomena in Focus*. Elsevier: Amsterdam, 1993.
7. Court H, Davies AR, Walters K. *Journal of non-Newtonian Fluid Mechanics* 1981; **8**:95.
8. Phan-Thien N, Tanner RI. *Journal of non-Newtonian Fluid Mechanics* 1977; **2**:353.
9. Crochet MJ, Davies AR, Walters K. *Numerical Simulation of non-Newtonian Flow*. Elsevier: Amsterdam, 1984.
10. Rallison J, Hinch EJ. *Journal of non-Newtonian Fluid Mechanics* 1988; **29**:37.
11. Baaijens FPT. *Journal of non-Newtonian Fluid Mechanics* 1998; **79**:361.
12. Tanner R. *Engineering Rheology* (2nd edn). Oxford University Press: Oxford, 2000.
13. Perera MGN, Walters K. *Journal of non-Newtonian Fluid Mechanics* 1977; **2**:49.
14. Perera MGN, Walters K. *Journal of non-Newtonian Fluid Mechanics* 1977; **2**:191.
15. Kawahara M, Takeuchi N. *Computers and Fluids* 1977; **5**:33.
16. Viriyayuthakorn M, Casewell B. *Journal of non-Newtonian Fluid Mechanics* 1980; **6**:245.
17. Bernstein B, Kadivar MK, Malkus DS. *Computer Methods in Applied Mechanical Engineering* 1981; **27**:279.
18. Townsend P. *Rheologica Acta* 1973; **12**:13.
19. Townsend P. *Journal of non-Newtonian Fluid Mechanics* 1984; **14**:265.
20. Davies AR, Devlin J. *Journal of non-Newtonian Fluid Mechanics* 1993; **50**:161.
21. Hinch EJ. *Journal of non-Newtonian Fluid Mechanics* 1993; **50**:161.
22. Renardy M. *Journal of non-Newtonian Fluid Mechanics* 1995; **58**:83.
23. Marchal JM, Crochet MJ. *Journal of non-Newtonian Fluid Mechanics* 1986; **20**:187.
24. Marchal JM, Crochet MJ. *Journal of non-Newtonian Fluid Mechanics* 1987; **26**:77.
25. Luo X-L, Tanner RI. *Journal of non-Newtonian Fluid Mechanics* 1989; **31**:143.
26. Yoo JY, Na Y. *Journal of non-Newtonian Fluid Mechanics* 1991; **39**:89.
27. Sato T, Richardson SM. *Journal of non-Newtonian Fluid Mechanics* 1994; **51**:249.
28. Basombrio FG, Buscaglia GC, Dari EA. *Journal of non-Newtonian Fluid Mechanics* 1991; **39**:189.

29. Baaijens FPT. *Computer Methods in Applied Mechanical Engineering* 1992; **94**:285.
30. Olsson F. *Journal of non-Newtonian Fluid Mechanics* 1994; **51**:309.
31. Aboubacar M, Webster MF. *International Journal for Numerical Methods in Fluids* 2003 in press.
32. Aboubacar M, Webster MF. *Journal of non-Newtonian Fluid Mechanics* 2001; **98**:83.
33. Basombrio FG, Buscaglia GC, Dari EA. *Journal of non-Newtonian Fluid Mechanics* 1990; **32**:11.
34. Fortin M, Fortin A. *Journal of non-Newtonian Fluid Mechanics* 1989; **32**:295.
35. Fortin M, Pierre R. *Journal of non-Newtonian Fluid Mechanics* 1989; **73**:341.
36. Keiller RA. *Journal of non-Newtonian Fluid Mechanics* 1993; **46**:143.
37. Purnode B, Crochet MJ. *Journal of non-Newtonian Fluid Mechanics* 1996; **65**:269.
38. Mitsoulis E. *Journal of non-Newtonian Fluid Mechanics* 1998; **78**:187.
39. Mitsoulis E. *Journal of non-Newtonian Fluid Mechanics* 2001; **97**:13.
40. Matallah H, Townsend P, Webster MF. *Journal of non-Newtonian Fluid Mechanics* 1998; **75**:139.
41. Baloch A, Townsend P, Webster MF. *Journal of non-Newtonian Fluid Mechanics* 1995; **59**:111.
42. Carew EOA, Townsend P, Webster MF. *Journal of non-Newtonian Fluid Mechanics* 1993; **50**:253.
43. Phillips TN, Williams AJ. *Journal of non-Newtonian Fluid Mechanics* 1999; **87**:215.
44. Alves MA, Pinho FT, Oliveira PJ. *Journal of non-Newtonian Fluid Mechanics* 2000; **93**:287.
45. Xue S-C, Phan-Thien N, Tanner RI. *Journal of non-Newtonian Fluid Mechanics* 1998; **74**:195.
46. Morton KW, Paisley MF. *Journal of Computational Physics* 1989; **80**:168.
47. Crumpton PI, MacKenzie JA, Morton KW. *Journal of Computational Physics* 1993; **109**:1.
48. Struijs R, Deconinck H, Roe PL. *Technical Report* 1990–01. Von Karman Institute of Fluid Dynamics, 1991.
49. Tomaich GT, Roe PL. *Modelling Simulation* 1993; **23**:2629.
50. Berzins M, Ware JM. *Applied Numerical Mathematics* 1995; **16**:417.
51. Wapperom P, Webster MF. *Journal of non-Newtonian Fluid Mechanics* 1998; **79**:405.
52. Wapperom P, Webster MF. *Computer Methods in Applied Mechanics and Engineering* 1999; **180**:281.
53. Chandio MS, Webster MF. *Proceedings of the 13th International Congress on Rheology*, Cambridge, UK, vol. 2, 2000; 208.
54. Xue S-C, Phan-Thien N, Tanner RI. *Journal of non-Newtonian Fluid Mechanics* 1995; **59**:191.
55. Huang X, Phan-Thien N, Tanner RI. *Journal of non-Newtonian Fluid Mechanics* 1996; **64**:71.

